Effects of El Niño Modoki on winter precipitation in Korea

Do-Woo Kim · Ki-Seon Choi · Hi-Ryong Byun

Abstract This study compares the impacts of El Niño Modoki and El Niño on precipitation over Korea during the boreal winters from 1954 to 2009. Precipitation in Korea tends to be equal to or greater than the normal level during an El Niño Modoki winter, whereas there is no significant change during an El Niño winter. Greater than normal precipitation during El Niño Modoki was also found over the lower reaches of the Yangtze River, China and much of southern Japan. The latitudes of these regions are 5–10° further north than in southern China, where precipitation increases during El Niño. The following two anomalous atmospheric circulations were found to be causes that led to different precipitation distributions over East Asia. First, an atmospheric wave train in the lower troposphere, which propagated from the central tropical Pacific (cyclonic) through the southern Philippine Sea (anticyclonic) to East Asia (cyclonic), reached the southern China and northern Philippine Sea during El Niño, whereas it reached Korea and southern Japan during El Niño Modoki. Second, an anomalous local meridional circulation, which consists of air sinking in the tropics, flowing poleward in the lower troposphere, and rising in the subtropics, developed between the southern Philippine Sea and northern Philippine Sea during El Niño. During El Niño Modoki, however, this circulation expanded further to the north and was formed between the southern Philippine Sea and regions of Korea and southern Japan.

Keywords El Niño Modoki · El Niño ·
Winter precipitation · Winter teleconnections ·
Anomalous local meridional circulation ·
Atmospheric wave train

D.-W. Kim
National Institute of Meteorological Research,
Korea Meteorological Administration, Seoul, Korea

K.-S. Choi
National Typhoon Center, Korea Meteorological Administration,
Jeju, Korea

H.-R. Byun (✉)
Department of Environmental Atmospheric Sciences,
Pukyong National University, 599-1 Daeyeon 3-dong,
Nam-gu, Busan 608-737, Republic of Korea
e-mail: hrbyun@pknu.ac.kr

1 Introduction

El Niño Modoki refers to a phenomenon in which the warm sea surface temperature (SST) develops in the central tropical Pacific with a colder SST on both its sides (the western and eastern tropical Pacific). This phenomenon is distinct from the canonical El Niño that is associated with warming in the eastern tropical Pacific (Ashok et al. 2007). Differences in the location and intensity of tropical heat sources during the canonical El Niño and El Niño Modoki lead to different patterns of global-scale atmospheric circulation (Larkin and Harrison 2005; Weng et al. 2007, 2009; Yeh et al. 2009). Therefore, compared with those of canonical El Niño, the precipitation anomalies during El Niño Modoki are quite different not only in the tropics but also in the extratropics. For example, during an El Niño Modoki (canonical El Niño) summer, western Japan and western USA are likely to be dry (wet), and during an El Niño Modoki (canonical El Niño) winter, southern China

and northwestern USA are likely to be dry (wet) (Weng et al. 2007, 2009). However, since the different teleconnection patterns of these two phenomena have only become known relatively recently, a more detailed analysis of their regional climate impacts remains a subject that requires additional research.

To study the impacts of El Niño Modoki on the winter climate over East Asia, we first need to understand the impacts of El Niño on East Asia and its mechanisms, which have been reported in previous studies. During an El Niño winter, a dipole pattern SST anomaly (SSTA) in the tropical Pacific causes anomalous single-cell Walker circulation, with an updraft over a wide area of the central-eastern Pacific and downdraft over the western Pacific (e.g., Klein et al. 1999; Wang 2002). This downdraft over the western Pacific, together with a local cold SSTA, develops an anomalous low-level anticyclone over the southern Philippine Sea. The southwesterlies on the western flank of this anticyclone bring warm, moist tropical air to East Asia (Wang et al. 2000). In addition, between the western tropical Pacific and East Asia, anomalous local meridional circulation develops, which consists of air sinking in the tropics, flowing poleward in the lower troposphere, rising in the subtropics, and returning back to the tropics in the upper troposphere (Wang 2002). These dynamics provide a favorable environment for increased precipitation over East Asia. Accordingly, in East Asian polar front regions from southern China to southern Japan via the East China Sea, a positive correlation appears between the intensity of El Niño and the amount of precipitation (Wang et al. 2000; Wu et al. 2003). The statistically significant region, however, is limited to southern China (Zhang et al. 1999; Wu et al. 2003). In the case of Korea, Cha et al. (1999) showed that precipitation in Korea increased slightly during an El Niño winter, while Kang (1998) reported that it is difficult to confirm a relationship between the two phenomena. Even though the analysis periods and the type of El Niño index used in the two studies are different, it can be noted that the impact of El Niño on winter precipitation in Korea is not very significant. However, the above studies that seek to understand the relationship between El Niño and precipitation over East Asia have considered a warm SSTA either in the eastern tropical Pacific or central tropical Pacific to be El Niño phenomena, without distinguishing between the canonical El Niño and El Niño Modoki. For example, they have often used the Nino 3.4 index as an El Niño index (Wang et al. 2000; Wu et al. 2003), even though this index represents signals of both the canonical El Niño and El Niño Modoki (Weng et al. 2007). To perform an accurate analysis therefore requires classification of the impacts of these two separate phenomena on winter precipitation over East Asia.

The impacts of El Niño Modoki on East Asian winter climate were partially revealed by Weng et al. (2009). A tripole pattern SSTA in the tropical Pacific during El Niño Modoki develops anomalous twin-cell Walker circulations, with an updraft over the central tropical Pacific and downdraft over both the western and eastern tropical Pacific. The downdraft over the western tropical Pacific is common during El Niño, but its center is located further north during El Niño Modoki. Accordingly, the anomalous low-level Philippine Sea anticyclone is also centered further north (over the South China Sea and the northern Philippine Sea). This means that the atmospheric circulation pattern over East Asia during El Niño Modoki is different from the pattern during El Niño. As a result, southern China and southern Japan, which are more likely to be wet during the canonical El Niño, tend to be dry during El Niño Modoki, though this phenomenon is not highly significant statistically. It is therefore necessary that researchers distinguish between the impacts of these two phenomena. However, in the observation data that Weng et al. (2009) used to analyze East Asian precipitation, the data for Korea are omitted. A large part of East Asia, including Korea, is in the western Pacific rim above 30°N, which is outside the region that receives the direct impacts of changes in the tropical Pacific SST (e.g., Diaz et al. 2001; Weng et al. 2009). Accordingly, in order to investigate the regional impacts of the canonical El Niño and El Niño Modoki on East Asia, it is meaningful to make a comparison by focusing on anomalous winters in which El Niño or El Niño Modoki developed strongly. A similar line of thinking was also advanced by Weng et al. (2007). The impacts of El Niño and El Niño Modoki on wintertime Southeast Asian rainfall have been revealed by Feng et al. (2010). They found that El Niño events generally favor below-normal rainfall across the Philippines, Borneo, Celebes, and Sulawesi and above-normal rainfall over south China. In contrast, for El Niño Modoki events, negative rainfall anomalies are generally observed in south China, the Indo-China peninsula, the Malay Peninsula, and the Philippines. They also suggested that the different Southeast Asian rainfalls during El Niño and El Niño Modoki are attributed to the different anomalous Walker circulation and low-level anticyclone around the Philippines.

In this study, through composite analyses of El Niño Modoki winters, the impacts of El Niño Modoki on winter precipitation over Korea were analyzed. These impacts were also compared with those of canonical El Niño winters. Although the boreal winter season in this study was defined as January, February and March, as in Weng et al. (2009), this study's analysis period covers 56 years (1954–2009), which is about twice as long as that of Weng et al. (1979–2005).

Fig. 1 a Locations of 13 weather stations used in this study. The *numbers* represent the station number. *Small circles* indicate location of 47 weather stations which have recorded data since 1973. **b** Annual time-series of winter mean precipitation averaged from 13 stations (since 1954) and from 47 stations (since 1973)
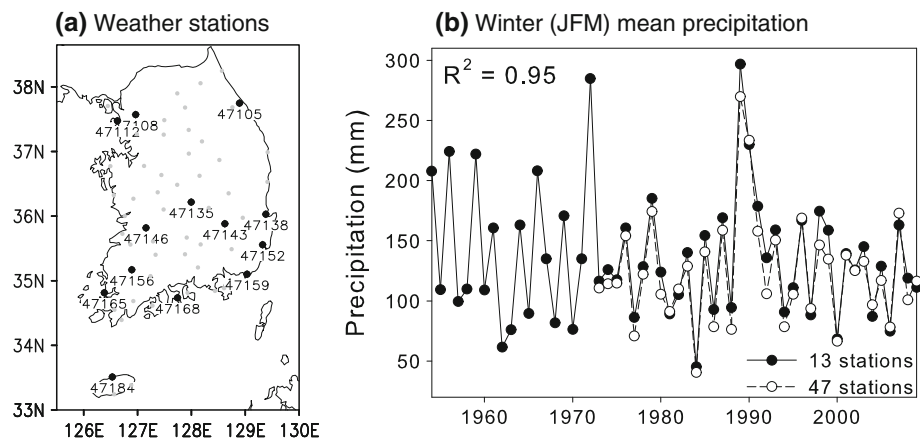
2 Data and methods

We used the precipitation data of 13 stations, which have been available since 1954 in Korea (Fig. 1a). Even though the 13 stations are not evenly distributed across the nation, the mean precipitation recorded by the 13 stations is a sufficient representative of the variation in mean precipitation of all 60 stations (available since 1973), which are evenly distributed across the nation (Fig. 1b). The 56-year mean winter precipitation of 13 stations is 135.9 mm and the standard deviation is 52.5 mm. The precipitation anomaly divided by the standard deviation was named as the standardized precipitation anomaly (SPA).

The Hadley Centre Global Sea Ice and Sea Surface Temperature (HadISST) Analyses datasets (Rayner et al. 2003) were used for SST analysis. The atmospheric data (wind, vertical velocity, velocity potential, geopotential, specific humidity, precipitable water content) were obtained from the National Center for Environmental Prediction/National Center for Atmospheric Research (NCEP/NCAR) reanalysis (Kalnay et al. 1996). Precipitation data from the Climate Research Unit (CRU) TS3 (Mitchell and Jones 2005) were used for the analysis of precipitation over East Asia (data covers up to 2006). The analysis period considered in this study covered the boreal winter seasons, composed of January–February–March (JFM), from 1954–2009. All the winter anomalies discussed in this paper are departures from their respective means for this period.

Following Ashok et al. (2007), the El Niño Modoki index (EMI) is defined as

$$EMI = [SSTA]_C - 0.5[SSTA]_E - 0.5[SSTA]_W,$$

where the square brackets with a subscript represent the area-mean SSTA over each of the three regions specified: the central region (C: 165°E–140°W, 10°S–10°N), the eastern region (E: 110°–70°W, 15°S–5°N), and the western region (W: 125°–145°E, 10°S–20°N). The index represents the zonal SST gradients in both the eastern and western tropical Pacific. The canonical El Niño is quantified by the NINO3 index (hereafter referred to as NINO3), which is defined by the area-mean SSTA over the region (150°–90°W, 5°S–5°N). These tropical regions are marked in Fig. 5. These indices were normalized by their standard deviation. In the following discussion, the term "El Niño" is generally used to refer to the canonical El Niño as defined by NINO3. Since EMI only considers zonal SST gradients, it may misidentify anomalous La Niña occurrences as El Niño Modoki occurrences. To avoid such misidentification, the NINO4 index (the area-mean SSTA over 160E°–150°W, 5°S–5°N) was used as subsidiary data.

Figure 2 presents a time series of the NINO3 and EMI. The linear correlation coefficient between the two indices is 0.4, which indicates some relationship between them. The correlation coefficient for each of the past 28 years (1954–1981) and for a more recent period (1982–2009) is 0.69 and 0.38, respectively, which indicates that the two indices are more independent of each other in the recent period than in the past.

3 Anomalies during El Niño and El Niño Modoki

3.1 Precipitation in Korea

Scatter plots of the standardized precipitation anomaly (SPA) in Korea based upon both NINO3 and EMI are represented in Fig. 3. It was considered that $-0.5 <$ SPA ≤ 0.5 represents a normal condition and $0.5 <$ SPA represents a wet condition. A linear relationship does not appear in either of the scatter plots. However, in cases when EMI is above 0.5, it is found that the scattering is inclined toward a wet condition. Among a total of 17 winters, 8 were wet, 8 were normal, and 1 was dry, indicating that during an El Niño Modoki, probability of drought over Korea is negligible.
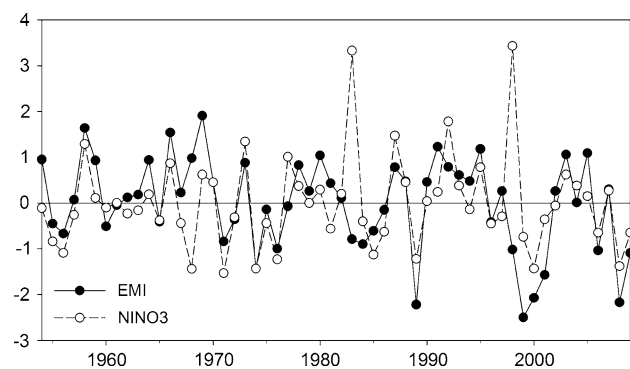
Fig. 2 Normalized time series of the mean NINO3 and EMI for Jan–Feb–Mar (JFM) for the period from 1954 to 2009

In 1968, which was the only dry winter among the 17 winters, the EMI value is 0.98 while the NINO3 and NINO4 values are −1.44 and −0.23, respectively. Thus, this winter is characterized by La Niña rather than El Niño Modoki. Except for 1968, all of the NINO4 values for 16 El Niño Modoki winters are positive. The average precipitation for the 16 El Niño Modoki winters is 155 mm, which exceeds the normal value (136 mm) by 19 mm. This difference is significant at an 80% confidence level. On the other hand, the average precipitation for the 16 El Niño winters is 132 mm, which is 4 mm less than the normal value.

There are winters in which both NINO3 and EMI have high positive values at the same time. In order to analyze the influence of El Niño and El Niño Modoki independently, El Niño winters and El Niño Modoki winters were redefined without duplicating them. Among 16 winters with an EMI over 0.5, the 12 winters in which the EMI ranking (in descending order out of 56 values) is higher than the NINO3 ranking were defined as El Niño Modoki winters (1954, 1958, 1959, 1964, 1966, 1969, 1978, 1980, 1991, 1995, 2003, and 2005). Similarly, among years with high NINO3 values, 12 winters in which the NINO3 ranking is higher than the EMI ranking were defined as El Niño winters (1970, 1973, 1977, 1982, 1983, 1987, 1988,

1992, 1993, 1998, 2004 and 2007). During the 12 El Niño Modoki winters, Korea was wet in 6 winters (50%) and was normal in the remaining 6 winters (50%). The average precipitation for the 12 winters was 151 mm, which exceeds the normal value by 15 mm (Fig. 4). The standard deviation of precipitation for the 12 winters was 36 mm. On the other hand, it was found that El Niño Modoki developed in only one winter among the five extremely wet winters (5 upper outliers found in the far left box plot) that have occurred during the entire 56-year analysis period. Therefore, the El Niño Modoki phenomenon is regarded as just one among a variety of climatic factors that influence winter precipitation in Korea, rather than being the outstanding climatic factor. On the contrary, during 12 El Niño winters, Korea was wet in 4 winters, normal in 4, and dry in 4, and the average rainfall was 126 mm, which is 6 mm less than the normal value. The standard deviation of precipitation for the 12 winters was 38 mm. Therefore, the impacts of El Niño on winter precipitation in Korea are quite small, which indicates an effect opposite to that of El Niño Modoki.

3.2 Sea surface temperature

In Fig. 5, we compare the composite of the SSTAs for the twelve El Niño events with those for the twelve El Niño Modoki events (Individual patterns can be found in the Electronic Supplementary Material, Fig. S1). During El Niño, there is a warm SSTA over the wide central-eastern tropical Pacific with a center near 130°W. The North and South Pacific Oceans are covered by cold SSTAs that are linked in the western tropical Pacific, forming a boomerang shape (cf. Trenberth and Stepaniak 2001). In particular, a cold SSTA is more prominent in North Pacific (cf. Schwing et al. 2002). These are typical characteristics that appear in the Pacific during El Niño. During El Niño Modoki, the SSTA pattern displays the following differences from that during El Niño. First, a tripole pattern SSTA is shown in the tropical Pacific, with warm SSTA in the central tropical Pacific and cold SSTA in the western and eastern tropical

Fig. 3 Scatter diagram for **a** NINO3, and **b** EMI and the standardized precipitation anomaly (SPA) of Korea. *Numerals* denote the last two digits of the year
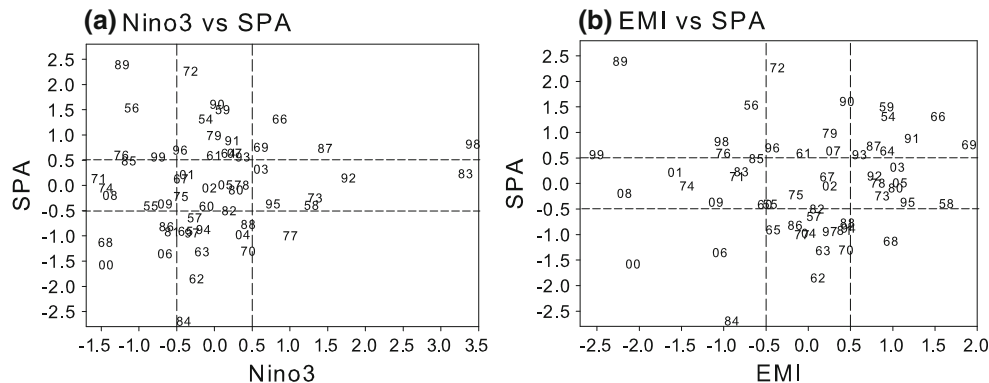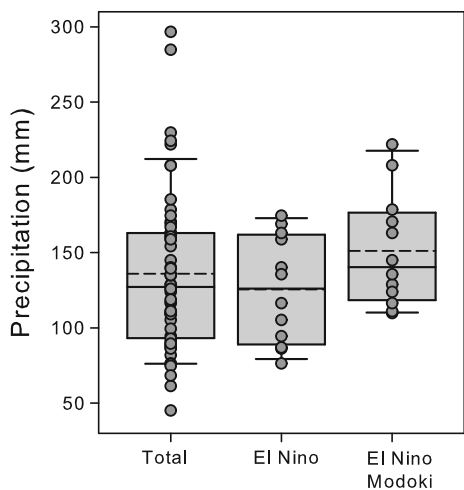
Fig. 4 *Box* plots of winter precipitation for 56 winters (1954–2009), 12 El Niño winters, and 12 El Niño Modoki winters. *Solid* and *dashed lines* in the *middle* of the *box denote* the average and the median, respectively

Pacific (e.g., Ashok et al. 2007; Weng et al. 2009). The warm SSTA extends to the southwestern USA. Second, the cold SSTA is more intensive over the western tropical Pacific near 140°E. Third, the cold SSTA in the North Pacific is weaker and shifts southeastward near (30°N, 140°W). These characteristics are almost consistent with the results reported by Weng et al. (2009).

3.3 Precipitation over East Asia

Precipitation teleconnection patterns associated with El Niño and El Niño Modoki were analyzed using precipitable water content data and CRU precipitation data (Fig. 6). Because CRU datasets covers up to 2006, the composite

map of CRU precipitation for El Niño (Fig. 6c) was consisted of 11 years, excepting 2007. As was discussed in Sect. 3.1, the increase in precipitation in Korea during an El Niño Modoki winter is not very significant. Thus, areas with confidence level over 80% were emphasized in the precipitation anomaly composite map. During El Niño (Fig. 6a), the wet anomaly is broadly distributed in the central-eastern topical Pacific, and the dry anomaly encompasses north-west-south circumference of the wet anomaly. This pattern is consistent with El Niño's SSTA pattern. Another characteristic is that a meridional wave train with alternating wet and dry anomalies extends from the central tropical Pacific through the southern Philippine Sea to the northern Philippine Sea and southern China (hereafter referred to as the tropical Pacific–East Asia wave train). During El Niño Modoki (Fig. 6b), in correspondence with the tropical Pacific SSTA pattern, the wet anomaly in the tropical Pacific exhibits a smaller zonal scale than the anomaly during El Niño. On the other hand, the tropical Pacific–East Asia wave train pattern extends further northward to Korea and southern Japan, at latitudes that are 5–10° higher than during El Niño.

Compared to during El Niño, the northward shift of the wet region over East Asia during El Niño Modoki is also confirmed by CRU precipitation data (Fig. 6c and d, individual patterns can be found in the Electronic Supplementary Material, Fig. S2). During El Niño, an apparent increase in precipitation is found over southern China. On the contrary, a decrease in precipitation is seen over Korea, Japan except the far southern region, and northern China above approximately 33°N. During El Niño Modoki, there is a reduction in the amount of precipitation increase in southern China; even decreases are seen in some regions, and its location shifts about 5° to the north into the lower
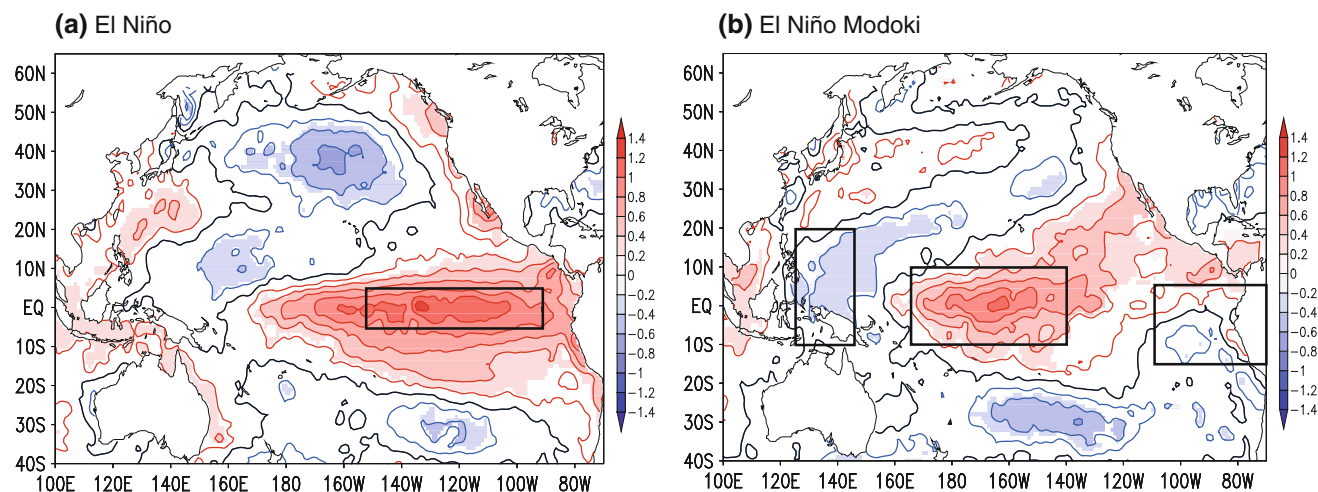

Fig. 5 Composites of SSTA (°C) for the twelve **a** El Niño, and **b** El Niño Modoki winters (JFM). Significant values above a 90% confidence level from a two-tailed student's *t*-test are *shaded*. The SSTAs in the *black boxes* in the panels are used to define the respective indices
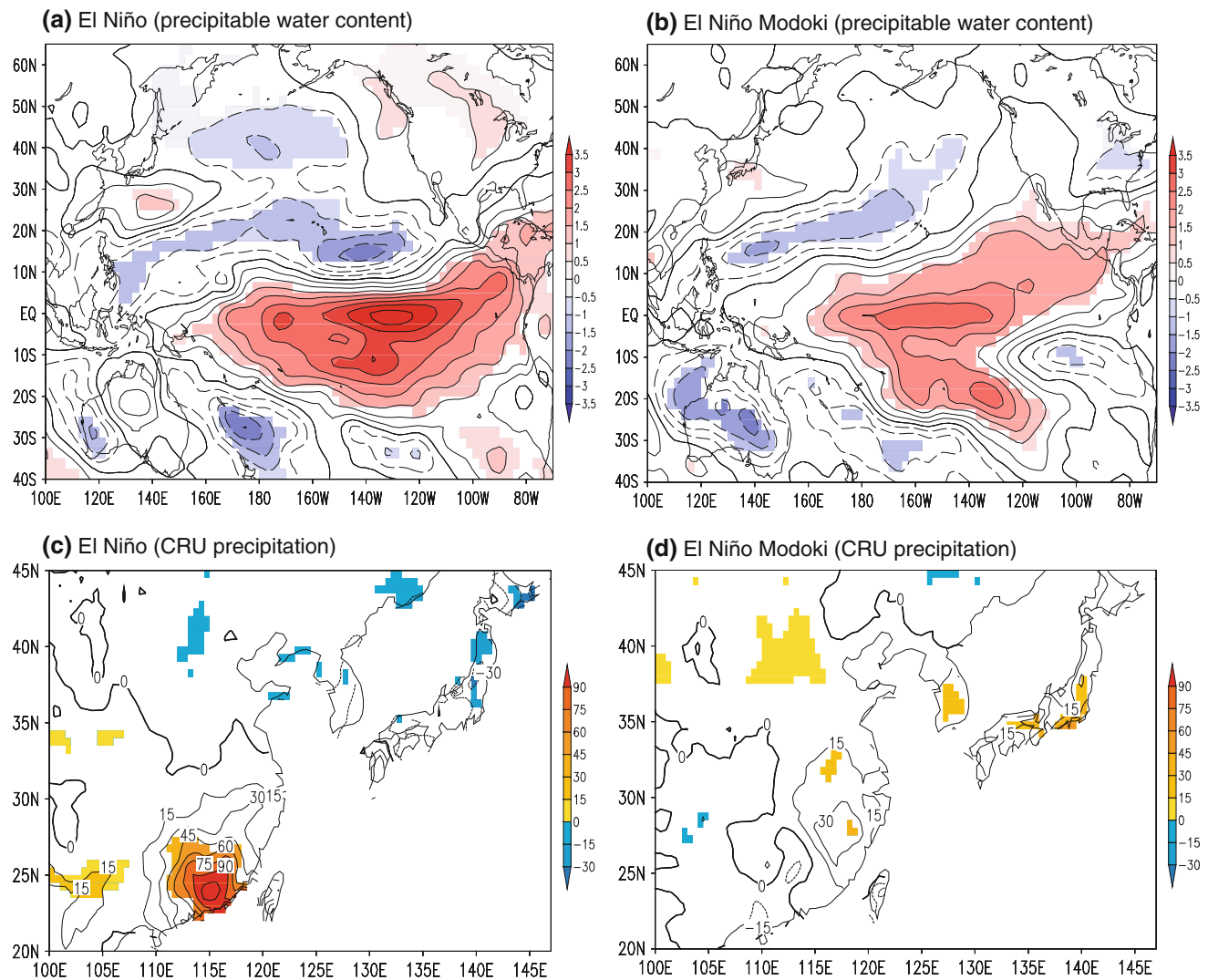
Fig. 6 Composites of **a**, **b** precipitable water content (kg m^{-2}), and **c**, **d** CRU precipitation anomalies for the (**a**, **c**) El Niño, and (**b**, **d**) El Niño Modoki winters (JFM). Significant values above a 90% confidence level from a two-tailed student's *t* test are *shaded*

reaches of the Yangtze River area. In addition, a significant increase in precipitation is found in Korea and much of southern Japan, which is a condition opposite to that of an El Niño winter. The responses to these two phenomena over southern China are similar to the results of Weng et al. (2009), whereas those over Japan display almost opposite results. The reason for this difference may be that Japan possibly lies outside the area impacted directly by El Niño and El Niño Modoki, as mentioned in the Introduction. Weng et al. (2009) revealed linear relationships between amount of precipitation and intensities of the two phenomena, hence in their results, effects of all kinds of El Niño events during the analysis period were considered, including not only La Niña and La Niña Modoki but normal conditions as well. This could be responsible for the

difference in our results, which focus only on El Niño and El Niño Modoki events.

4 Teleconnection paths

4.1 Horizontal atmospheric circulations

Figure 7 shows upper and lower tropospheric circulation anomaly composites for the twelve El Niño events and for the twelve El Niño Modoki events. In upper troposphere during El Niño (Fig. 7a), symmetrical anticyclonic circulation anomalies cover both the subtropical North and South Pacific Oceans. To the north, a cyclonic circulation anomaly over the northern North Pacific and an
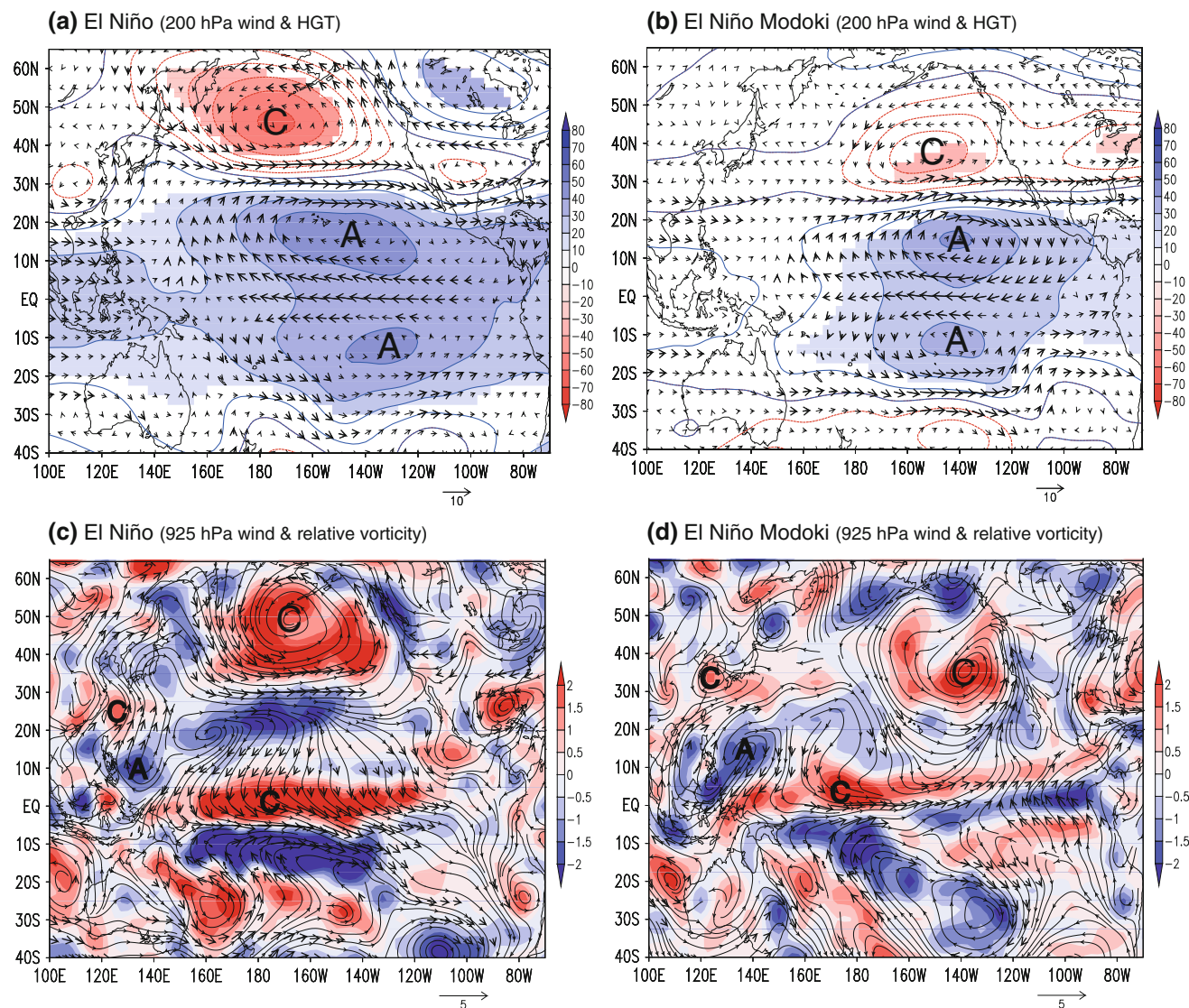
Fig. 7 Composites of **a**, **b** 200 hPa geopotential height (*shading*, unit: gpm) and wind anomalies, and **c**, **d** 925 hPa relative vorticity (*shading*, unit: $10^{-5}\ s^{-1}$) and wind anomalies for the twelve **a**, **c** El Niño and **b**, **d** El Niño Modoki winters (JFM). Significant values above a 90% confidence level are *shaded* in (**a**, **b**). The *bold* vector represents a significant wind anomaly above a 90% confidence level

anticyclonic circulation anomaly over northern North America are found. These anomalies represent the arching wave train patterns forced by tropical heat sources during El Niño (Wallace and Gutzler 1981; Trenberth et al. 1998), and they are similar to the positive phase of the classical Pacific-North American (PNA) teleconnection pattern (Horel and Wallace 1981). During El Niño Modoki (Fig. 7b), symmetrical anomaly patterns are also found over both the subtropical North and South Pacific Oceans, but on a reduced scale compared to those found during El Niño. Corresponding to the smaller-scale anticyclonic circulation anomaly over the subtropical North Pacific, the cyclonic circulation anomaly over the extra tropical North Pacific also appears weaker, with its center shifted southeastward. The reason that anomalous atmospheric

circulations exhibit smaller spatial scales during El Niño Modoki than during El Niño may be that the warm SST area in the tropical Pacific, which forces the atmospheric teleconnection pattern, is smaller during El Niño Modoki (Bulic and Brankovic 2007).

During El Niño, the cyclonic circulation anomaly over the northern North Pacific is found in the lower (Fig. 7c) as well as the upper level. The superposition of an eastward flow on the southern flank of this cyclone on the midlatitude climatological westerly wind would lead to an increase in wind speed, and thus to cooling of the SST in the central North Pacific (See Fig. 5a). This process is the most typical phenomenon appearing in the North Pacific during El Niño (Lau 1997; Alexander et al. 2002). On the other hand, the central tropical Pacific–East Asia wave
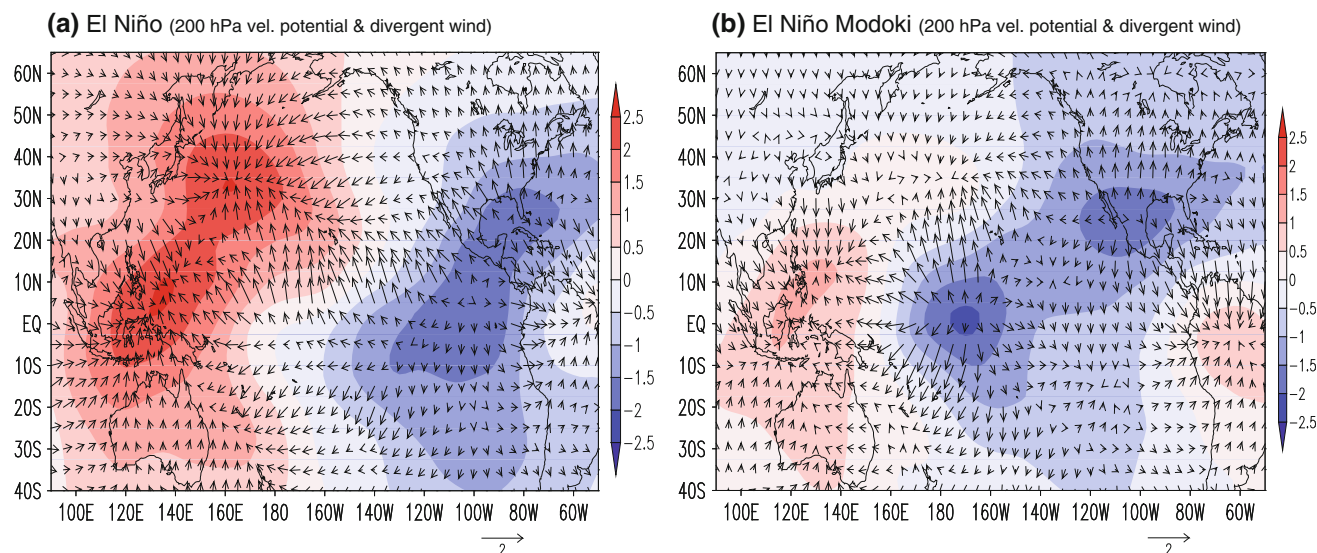
Fig. 8 Composites of 200 hPa divergent winds (*arrow*) and velocity potential (*shaded*, units: 10^6 m^2 s^{-1}) anomalies for the twelve **a** El Niño and **b** El Niño Modoki winters (JFM)

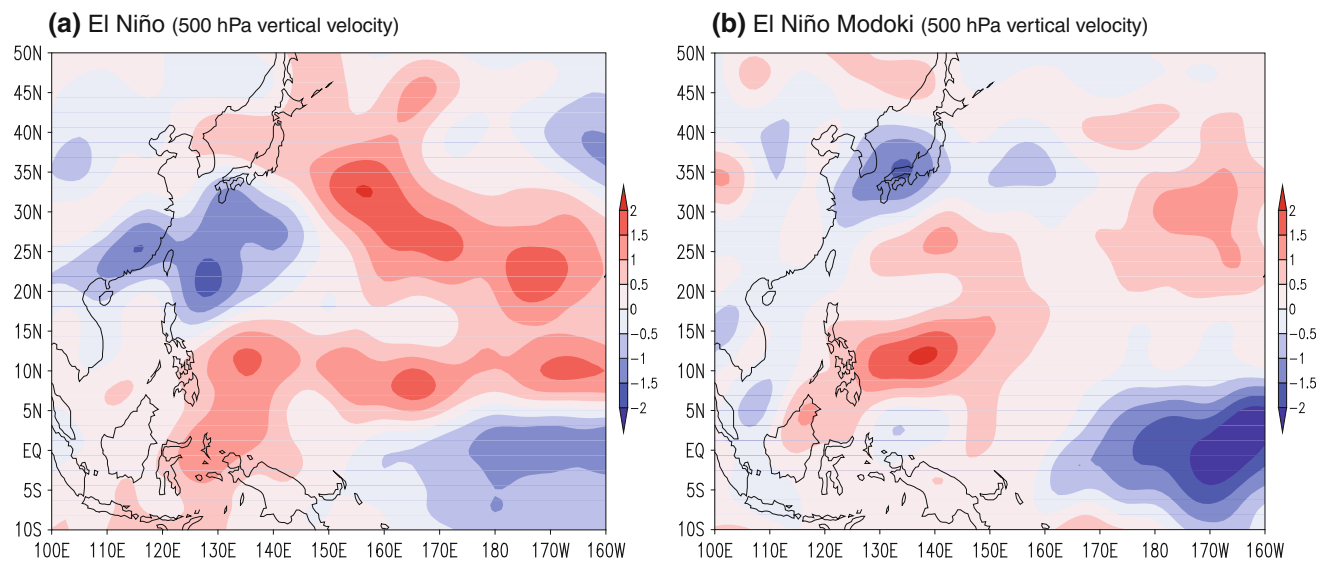**Fig. 9** Composites of 500 hPa vertical velocity (10^{-2} Pa s^{-1}) for the twelve **a** El Niño and **b** El Niño Modoki winters (JFM)

train that appeared in the precipitable water content anomaly field is again confirmed in the lower troposphere, which consists of a cyclonic anomaly in the central tropical Pacific, an anticyclonic anomaly in the southern Philippine Sea, and a cyclonic anomaly in the northern Philippine Sea and southern China. This plays an important role in propagating the impacts of heat sources in the tropical Pacific on East Asia (Wang et al. 2000). During El Niño Modoki, in the lower troposphere (Fig. 7d), intensity of the relative vorticity anomalies is weaker as a whole and statistically significant wind anomalies also appear more regionally. In particular, the cyclonic circulation anomaly over the North Pacific is weaker and is located further southeast than it is

during El Niño. This may result in a relatively less cold SSTA in the North Pacific during El Niño Modoki than during El Niño (See Fig. 5b). On the other hand, it is notable that the northern edge of the anticyclonic vorticity anomaly over the Philippine Sea reaches up to 25°N, which is about 5° further north than it reaches during El Niño. A similar result has been shown by Feng et al. (2010). They simulated atmospheric circulations during the El Niño and El Niño Modoki events using a simple baroclinic model and suggested that the different patterns of the Philippine anticyclone result from the difference in the diabatic heating associated with the two types of Pacific Ocean warming. As the anticyclonic circulation anomaly shifts

further north, the tropical Pacific-East Asia wave train reaches up to Korea and southern Japan.

4.2 Vertical atmospheric circulations

Figure 8a, b show the anomalous upper-level velocity potential and divergent winds related to both El Niño and El Niño Modoki, which indicate how upper-level air flows from the mass sources to sinks. During El Niño (Fig. 8a) a dipole pattern anomalies is visible, with an upper-level mass sink (convergence) over the western Pacific and an upper-level mass source (divergence) over the eastern Pacific. These anomaly patterns are related to the weakening of Walker circulation (Weng et al. 2009). In a broad mass sink area over the western Pacific, there are two centers. The first one, which is located over the southern Philippine Sea, is related to the descending branch of the anomalous Walker circulation. The second one is over the eastern ocean of Japan, where northwesterlies and southwesterlies converge, respectively, from upper-level cyclonic circulation over the northern North Pacific and upper-level anticyclonic circulation over the subtropical North Pacific (See Fig. 7a). These dynamics are consistent with the El Niño pattern shown in previous studies (Mestas-Nuñez and Enfield 2001; Wang 2002; Weng et al. 2009). Over Southeast Asia to the north of the equator, anomalous northerly divergent winds are prominent, flowing toward the center of an upper-level mass sink over the southern Philippine Sea, while over East Asia above 30°N, anomalous westerly divergent winds are dominant, flowing toward the center of an upper-level mass sink over the eastern ocean of Japan. Over the East China Sea and northern Philippine Sea, divergent winds disperse toward

the centers of both mass sinks. During an El Niño Modoki (Fig. 8b), a tripole type of pattern over the tropics is noticed, with an upper-level mass source over the central tropical Pacific and upper-level mass sinks over the southern Philippine Sea and northern South America. This pattern is associated with the anomalous two-cell Walker circulation (Weng et al. 2009). On the other hand, it is found that the upper-level mass sink that appeared clearly in the eastern ocean of Japan during El Niño, is so weak as to be almost indistinguishable during El Niño Modoki, and its location also shifts toward the east. Over East Asia above 30°N, there is a weak upper-level mass source anomaly, which is a condition opposite to that over Southeast Asia. Accordingly, anomalous northerly divergent winds flow from Korea and southern Japan to the southern Philippine Sea.

The anomalous vertical velocity field at 500 hPa over the western Pacific rim for El Niño and El Niño Modoki is shown in Fig. 9. During El Niño (Fig. 9a), there is an anomalous descent over the southern Philippine Sea, which corresponds to the upper-level mass sink there. On the contrary, there is an anomalous ascent over the southern China and northern Philippine Sea, where upper-level divergent winds dispersed toward the two mass sinks center over the southern Philippine Sea and the eastern ocean of Japan. This meridional dipole pattern of vertical velocity anomalies implies that an anomalous local meridional circulation forms between the southern Philippine Sea and northern Philippine Sea. During El Niño Modoki (Fig. 9b), as well as during El Niño, there is an anomalous descent over the southern Philippine Sea that corresponds to the upper-level mass sink; however, the area is located further north and includes the northern Philippine Sea.
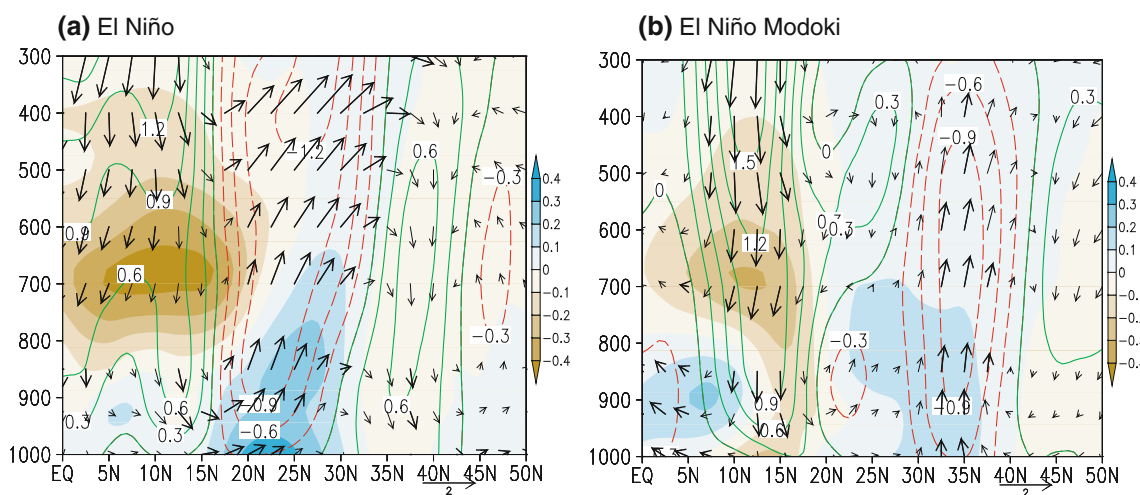

Fig. 10 Composite latitude-height cross-section of vertical velocity, meridional wind speed, and specific humidity anomalies along 120–140°E for the twelve **a** El Niño and **b** El Niño Modoki winters (JFM). The contour represents vertical velocity anomalies (10^{-2} Pa s^{-1}). Specific humidity anomalies (g kg^{-1}) are *shaded*. The *bold* vector represents a significant wind anomaly above a 90% confidence level

Accordingly, its counterpart, i.e., anomalous ascent is found over Korea and southern Japan, where its latitude is 5–10° further north than it is during El Niño. This is consistent with the northward extension of the tropical Pacific-East Asia low-level wave train pattern shown in Fig. 7d.

Figure 10 shows a composite of the latitude-pressure cross-section of vertical flow averaged along 120–140°E, which is the longitude belt that includes Korea and southern Japan (Individual patterns can be found in the Electronic Supplementary Material, Fig. S3a and S3b). During El Niño (Fig. 10a), a dry downdraft is dominant in the 0°–15°N region (the southern Philippine Sea). Its counterpart of wet updraft appears significantly in the 15°–30°N region (the northern Philippine Sea), and in the lower troposphere, an inflow of tropical air appears. A downdraft is also seen in the higher latitude region above 30°N but it does not have a high level of statistical significance. This means that the influence of El Niño on East Asia through anomalous local meridional circulation is limited to south of 30°N. Thus, Korea is located outside the El Niño impact zone. During El Niño Modoki (Fig. 10b), a dry downdraft is also dominant over the southern Philippine Sea. However, its counterpart, i.e., updraft is seen in higher latitudes centered at 30°–35°N (Korea and southern Japan). Thus during an El Niño Modoki, the pattern appears to shift northward by about 10° (comparing Fig 10a, b). This is a favorable atmospheric environment for the formation of precipitation over Korea.

5 Concluding remarks and discussions

This study has analyzed the impacts of El Niño Modoki phenomena on winter precipitation in Korea during the boreal winters (January, February and March) from 1954 to 2009. The study also compared how these impacts differed from those of the El Niño phenomenon. As a result, it was found that precipitation in Korea tends to be equal to or greater than the normal level during El Niño Modoki winters; among 12 El Niño Modoki winters, Korea was wet in 6 winters and normal in the other 6. Even though it does not have a high level of statistical significance, this teleconnection shows a greater degree of relationship than was found in previous studies (Kang 1998; Cha et al. 1999; Kim et al. 2008), which considered the expanded concept of "El Niño" without distinguishing between El Niño and El Niño Modoki. In addition, we found that precipitation in Korea is likely to decrease a little under the influence of El Niño alone, apart from that of El Niño Modoki, though it does not reach a significant level. This finding does not agree with that of Cha et al. (1999), who suggested that El Niño could lead to wet conditions in Korea.

An increase in precipitation during El Niño Modoki occurred not only over Korea but also over the lower reaches of the Yangtze River, China and much of southern Japan. Normally the rainfall variations over the Yangtze River, Korea, and southern part of Japan are in phase during summer (Kripalani and Kulkarni 2001). These regions are 5–10° further north in latitude than southern China, where precipitation increases during El Niño.

Figure 11 shows a schematic illustration of anomalous atmospheric circulations during El Niño and El Niño Modoki, which lead to different precipitation teleconnection patterns over East Asia. During both phenomena, a low-level wave train extends from the central Pacific (cyclonic) through the Philippine Sea (anticyclonic) to East Asia (cyclonic). During El Niño Modoki, however, the
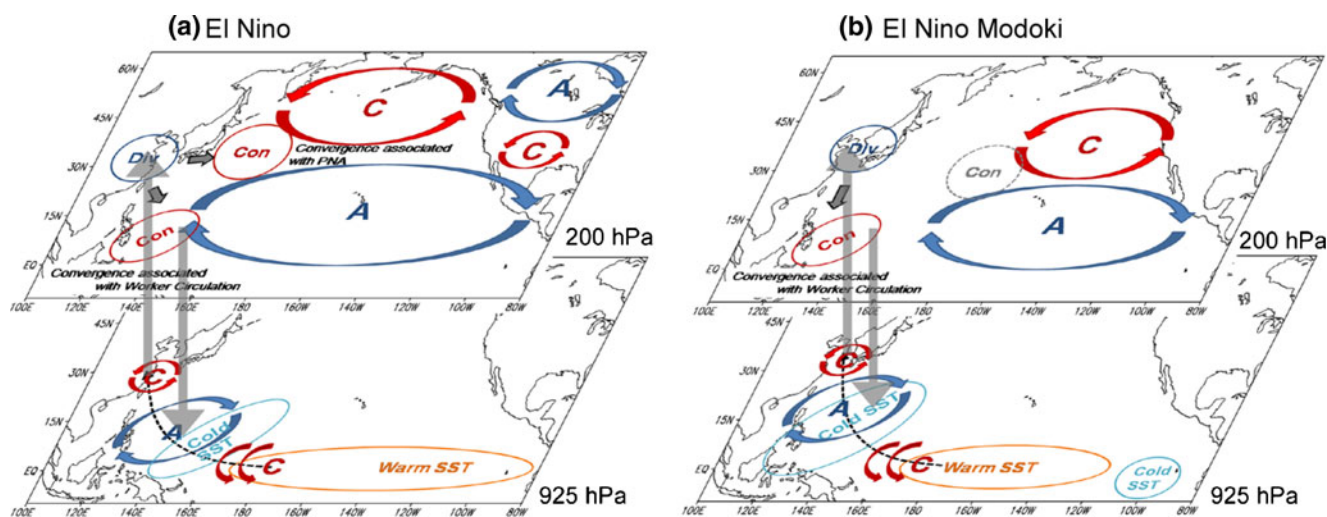

Fig. 11 Schematic illustration of anomalous atmospheric circulation patterns during **a** El Niño, and **b** El Niño Modoki: "*A*": anticyclonic flow, "*C*": cyclonic flow, *dashed arrow* at 925 hPa: low-level wave train, *vertical arrow*: atmospheric vertical motion, *gray arrow* at 200 hPa: divergent wind component, "*Con*" convergence, "*Div*" divergence

center of anomalous low-level anticyclonic circulation shifts north to the northern Philippine Sea. Due to this difference, the low-level wave train reaches up to Korea and southern Japan during El Niño Modoki, whereas it reaches only up to the southern China and northern Philippine Sea during El Niño. There are also clear differences between the two phenomena in terms of upper layer atmosphere circulation. During El Niño, Walker circulation becomes weak over the tropical Pacific and a PNA pattern develops over the North Pacific. Associated with these, an upper-level convergence zone that has two centers develops broadly over the western Pacific. The first center is over the southern Philippine Sea, where a descending branch of the anomalous Walker circulation develops. The second center is over the eastern ocean of Japan, and is associated with the PNA pattern. Between these two upper-level convergence centers, an upper-level divergence component forms over the northern Philippine Sea, where it can facilitate the development of ascending airflow, which compensates for the descending airflow over the southern Philippine Sea. Consequently, in the longitudes where the Korean Peninsula is located (120°–140°E), anomalous local meridional circulation develops, which consists of ascent over the northern Philippine Sea and descent over the southern Philippine Sea. Korea, however, is located outside of its impact area. During El Niño Modoki, as well as during El Niño, the first upper-level convergence center related to anomalous Walker circulation appears in the southern Philippine Sea. However, the second upper-level convergence center that develops over the eastern ocean of Japan during El Niño almost does not develop, and is located far to the southeast. The reason for this seems to be that anomalous atmospheric circulation develops on a smaller scale during El Niño Modoki than during El Niño, and this is associated with a smaller zonal-scale SSTA during El Niño Modoki. These anomalous upper-level atmosphere circulations provide an environment in which an upper-level divergence zone corresponding to the upper-level convergence over the southern Philippine Sea can be formed at higher latitude during El Niño Modoki than during El Niño. As a result, anomalous local meridional circulation is formed, with a downdraft over the southern Philippine Sea and an updraft over Korea and southern Japan. This corresponds well to the movement to the north of the tropical Pacific-East Asia low-level wave train during El Niño Modoki. Over Korea, an increased inflow of tropical air in the lower troposphere and the enhanced updraft provide a favorable environment for an increase in precipitation.

This study explains qualitatively the cause of teleconnection between El Niño Modoki and Korean winter precipitation. If, in the future, the impacts of the intensities of a warm SST in the central Pacific and cold SST in the western and eastern Pacific on the teleconnection pattern between El Niño Modoki and the East Asian climate are quantitatively analyzed by numerical studies, we can expect that our understanding of the El Niño Modoki teleconnection will be enhanced.

References

Alexander MA, Blade I, Newman M, Lanzante JR, Lau NC, Scott JD (2002) The atmospheric bridge: the influence of ENSO teleconnections on air–sea interaction over the global oceans. J Clim 15:2205–2231

Ashok K, Behera S, Rao AS, Weng HY, Yamagata T (2007) El Nino Modoki and its teleconnection. Geophys Res Lett 112:C11007. doi:10.1029/2006JC003798

Bulic IH, Brankovic C (2007) ENSO -forcing of the northern hemisphere climate in a large ensemble of model simulations based on a very long SST record. Clim Dyn 28:231–254

Cha EJ, Jhun JG, Chung HS (1999) A study on characteristics of climate in South Korea for El Nino/La Nina Years. Asia-Pacific J Atoms Sci 35:98–117 (In Korean with English abstract)

Diaz HF, Hoerling MP, Eischeid JK (2001) ENSO variability, teleconnections and climate change. Int J Climatol 21:1845–1862

Feng J, Wang L, Chen W, Fong SK, Leong KC (2010) Different impacts of two types of Pacific Ocean warming on Southeast Asian rainfall during boreal winter. J Geophys Res 115:D24122. doi:10.1029/2010JD014761

Horel J, Wallace JM (1981) Planetary scale phenomena associated with the Southern Oscillation. Mon Wea Rev 109:813–829

Kalnay E, Kanamitsu M, Kistler R, Collins W, Deaven D, Gandin J, Iredell M, Saha S, White G, Wollen J, Zhu Y, Chelliah M, Ebisuzaki W, Higgins W, Janowiak J, Mo KC, Ropelewski C, Wang J, Leetmaa A, Reynolds R, Jenne R, Joseph D (1996) The NCEP/NCAR 40-year reanalysis project. Bull Am Meteor Soc 77:437–471

Kang IS (1998) Relationship between El-Nino and Korean climate variability. Asia-Pacific J Atoms Sci 34:390–396 (In Korean with English abstract)

Kim YH, Kim MK, Lee WS (2008) An investigation of large-scale climate indices with the influence on temperature and precipitation variation in Korea. Atmosphere 18:83–95 (In Korean with English abstract)

Klein SA, Soden BJ, Lau NC (1999) Remote sea surface temperature variations during ENSO: evidence for a tropical atmospheric bridge. J Clim 12:917–932

Kripalani RH, Kulkarni A (2001) Monsoon rainfall variations and teleconnections over South and East Asia. Int J Climatol 21:603–616

Larkin NK, Harrison DE (2005) Global seasonal temperature and precipitation anomalies during El Nino autumn and winter. Geophys Res Lett 32:L16705. doi:10.1029/2005GL022860

Lau NC (1997) Interactions between global SST anomalies and the midlatitude atmospheric circulation. Bull Am Meteor Soc 78:21–33

Mestas-Nuñez AM, Enfield DB (2001) Eastern equatorial Pacific SST variability: ENSO and non-ENSO components and their climatic associations. J Clim 14:391–402

Mitchell TD, Jones PD (2005) An improved method of constructing a database of monthly climate observations and associated high-resolution grids. Int J Climatol 25:693–712

Rayner NA, Parker DE, Horton EB, Folland CK, Alexander LV, Rowell DP, Kent EC, Kaplan A (2003) Global analyses of sea surface temperature, sea ice, and night marine air temperature since the late nineteenth century. J Geophys Res 108:4407. doi:10.1029/2002JD002670

Schwing FB, Murphree T, Dewitt L, Green PM (2002) The evolution of oceanic and atmospheric anomalies in the northeast Pacific during the El Niño and La Niña events of 1995–2001. Prog Ocean 54:459–491

Trenberth KE, Stepaniak DP (2001) Indices of El Nino evolution. J Clim 14:1697–1701

Trenberth KE, Branstator GW, Karoly D, Kumar A, Lau NC, Ropelewski C (1998) Progress during TOGA in understanding and modeling global teleconnections associated with tropical sea surface temperatures. J Geophys Res 103:14291–14324

Wallace JM, Gutzler DS (1981) Teleconnections in the geopotential height field during the northern hemisphere winter. Mon Wea Rev 109:784–812

Wang C (2002) Atmospheric circulation cells associated with the El Nino-Southern Oscillation. J Clim 15:399–419

Wang B, Wu R, Fu X (2000) Pacific-East Asian teleconnection: How does ENSO affect East Asian climate? J Clim 13:1517–1536

Weng H, Ashok K, Behera SK, Rao SA, Yamagata T (2007) Impacts of recent El Niño Modoki on dry/wet conditions in the Pacific rim during boreal summer. Clim Dyn 29:113–129

Weng H, Behera SK, Yamagata T (2009) Anomalous winter climate conditions in the Pacific rim during recent El Niño Modoki and El Niño events. Clim Dyn 32:663–674

Wu R, Hu ZZ, Kirtman BP (2003) Evolution of ENSO-related rainfall anomalies in East Asia and the processes. J Clim 16:3742–3758

Yeh SW, Kug JS, Dewitte B, Kwon MH, Kirtman BP, Jin FF (2009) El Niño in a changing climate. Nature 461:511–514

Zhang R, Sumi A, Kimoto M (1999) A diagnostic study of the impact of El Nino on the precipitation in China. Adv Atmos Sci 16:229–241